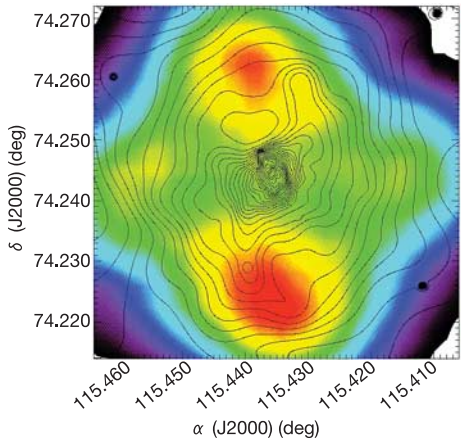

Figure 4 Temperature map of the central 200 × 200 arcsec of the cluster. Redder colours indicate hotter temperatures. The logarithmically spaced contours, ranging in surface brightness from $1\sigma = 1.0^{-4}$ counts s^{-1} cm^{-2} $pixel^{-2}$ to 100σ, show the locations of the cavities. The hottest regions are at the tips of the cavities, where the shocks are strongest.

use of X-ray temperature and luminosity functions to probe the large-scale structure and cosmology[22].

The huge proportion of this event suggests that it was powered by accretion onto a black hole. Equating the shock energy to $0.1\,Mc^2$ gives an estimate of the minimum accreted mass required to power the burst of $M \simeq 3\times10^8 M_\odot$, itself the mass of a supermassive black hole. The relationship between galactic-bulge luminosity and black-hole mass[23] predicts that a $\sim 10^9 M_\odot$ black hole resides there (assuming the cD galaxy's absolute visual magnitude within a 35-kpc diameter is −22.4; ref. 24). The central black hole evidently accreted a substantial fraction of its own mass in only 10^8 yr, a remarkable growth rate for such a large black hole. Although a similar line of reasoning would apply to quasars, their ages and average jet powers have not been measured directly. Such a rapid rate of growth may be difficult to reconcile with the small scatter in the relation of the black-hole mass to the bulge mass[25], and is at variance with the view that the most massive black holes have evolved slowly in the recent past[26].

Finally, the magnetic field strengths in clusters are typically a few microgauss[27], and evidence is growing for the existence of large-scale, intergalactic fields[28,29]. These fields could be generated and dispersed by outflows from supermassive black holes[28,29]. The equivalent magnetic field strength corresponding to the energy density within the cavities is $\sim$100 μG, considerably larger than the accumulated field strengths in clusters[27]. Therefore, a plausibly small fraction of the total energy of this one radio outburst alone, if channelled into the cluster's magnetic field, would magnetize the cluster. □

Received 17 August; accepted 12 November 2004; doi:10.1038/nature03202.

1. Fabian, A. C. Cooling flows in clusters of galaxies. *Annu. Rev. Astron. Astrophys.* **32,** 277–318 (1994).
2. Peterson, J. R. *et al.* High-resolution X-ray spectroscopic constraints on cooling-flow models for clusters of galaxies. *Astrophys. J.* **590,** 207–224 (2003).
3. Fabian, A. C., Mushotzky, R. F., Nulsen, P. E. J. & Peterson, J. R. On the soft X-ray spectrum of cooling flows. *Mon. Not. R. Astron. Soc.* **321,** L20–L24 (2001).
4. McNamara, B. R. *et al.* Chandra X-Ray Observations of the Hydra A cluster: An interaction between the radio source and the X-ray-emitting gas. *Astrophys. J. Lett.* **534,** 135–138 (2000).
5. Bîrzan, L. *et al.* A systematic study of radio-induced X-ray cavities in clusters, groups, and galaxies. *Astrophys. J.* **607,** 800–809 (2004).
6. Fabian, A. C. *et al.* A deep Chandra observation of the Perseus cluster: shocks and ripples. *Mon. Not. R. Astron. Soc.* **344,** 43–47 (2003).
7. Forman, W. *et al.* Reflections of AGN outbursts in the gaseous atmosphere of M87. *Astrophys. J.* (in the press).
8. Soker, N. *et al.* A moderate cluster cooling flow model. *Astrophys. J.* **549,** 832–839 (2001).
9. Nulsen, P. E. J. *et al.* The cluster-scale AGN outburst in Hydra A. *Astrophys. J.* (submitted).
10. Scheuer, P. A. G. Models of extragalactic radio sources with a continuous energy supply from a central object. *Mon. Not. R. Astron. Soc.* **166,** 513–528 (1974).
11. Heinz, S., Reynolds, C. S. & Begelman, M. C. X-ray signatures of evolving radio galaxies. *Astrophys. J.* **501,** 126–136 (1998).
12. Condon, J. J. *et al.* The NRAO VLA sky survey. *Astron. J.* **115,** 1693–1716 (1998).
13. Bicknell, G. V., Dopita, M. A. & O'Dea, C. P. Unification of the radio and optical properties of gigahertz peak spectrum and compact steep-spectrum radio sources. *Astrophys. J.* **485,** 112–124 (1997).
14. De Young, D. S. On the relation between Fanaroff-Riley types I and II radio galaxies. *Astrophys. J. Lett.* **405,** 13–16 (1993).
15. Donahue, M., Stocke, J. T. & Gioia, I. M. Distant cooling flows. *Astrophys. J.* **385,** 49–60 (1992).
16. Churazov, E. *et al.* Evolution of buoyant bubbles in M87. *Astrophys. J.* **554,** 261–273 (2001).
17. Churazov, E. *et al.* Cooling flows as a calorimeter of active galactic nucleus mechanical power. *Mon. Not. R. Astron. Soc.* **332,** 729–734 (2002).
18. Edge, A. C. The detection of molecular gas in the central galaxies of cooling flow clusters. *Mon. Not. R. Astron. Soc.* **328,** 762–782 (2001).
19. McNamara, B. R. & O'Connell, R. W. Star formation in cooling flows in clusters of galaxies. *Astron. J.* **98,** 2018–2043 (1989).
20. Donahue, M. & Stocke, J. T. *ROSAT* observations of distant clusters of galaxies. *Astrophys. J.* **449,** 554–566 (1995).
21. Wu, K. K. S., Fabian, A. C. & Nulsen, P. E. J. Non-gravitational heating in the hierarchical formation of X-ray clusters. *Mon. Not. R. Astron. Soc.* **318,** 889–912 (2000).
22. Markevitch, M. The LX-T relation and temperature function for nearby clusters revisited. *Astrophys. J.* **504,** 27–34 (1998).
23. Gebhardt, K. *et al.* A relationship between nuclear black hole mass and galaxy velocity dispersion. *Astrophys. J. Lett.* **539,** 13–16 (2000).
24. Stocke, J. T. *et al.* The Einstein Observatory extended medium-sensitivity survey. II—The optical identifications. *Astrophys. J. Suppl.* **76,** 813–874 (1991).
25. Ferrarese, L. & Merritt, D. A fundamental relation between supermassive black holes and their host galaxies. *Astrophys. J.* **539,** L9–L12 (2000).
26. Heckman, T. M. *et al.* Present-day growth of black holes and bulges: the SDSS perspective. *Astrophys. J.* **613,** 109–118 (2004).
27. Clarke, T. E., Kronberg, P. P. & Böhringer, H. A new radio-X-ray probe of galaxy cluster magnetic fields. *Astrophys. J. Lett.* **547,** 111–114 (2001).
28. Kronberg, P. P. *et al.* Magnetic energy of the intergalactic medium from galactic black holes. *Astrophys. J.* **560,** 178–186 (2001).
29. Furlanetto, S. R. & Loeb, A. Intergalactic magnetic fields from quasar outflows. *Astrophys. J.* **556,** 619–634 (2001).

Acknowledgements B.R.McN. thanks G. Evrard, D. De Young, M. Sharma and J. Shields for discussions. The National Radio Astronomy Observatory is operated by Associated Universities Inc., under cooperative agreement with the National Science Foundation. This work was supported by a NASA Long Term Space Astrophysics grant, a Chandra Archival Research grant, a Chandra Guest Observer grant, and a contract from the Department of Energy through the Los Alamos National Laboratory.

Competing interests statement The authors declare that they have no competing financial interests.

Correspondence and requests for materials should be addressed to B.R.McN. (mcnamarb@ohio.edu).

Quantized conductance atomic switch

K. Terabe[1,2], T. Hasegawa[1,2,3], T. Nakayama[1,2,3] & M. Aono[1,2,3]

[1]*Nanomaterials Laboratories, National Institute for Materials Science, 1-1 Namiki, Tsukuba, Ibaraki 305-0044, Japan*
[2]*ICORP-SORST/Japan Science and Technology Agency, 4-1-8 Honcho, Kawaguchi, Saitama 332-0012, Japan*
[3]*RIKEN, 2-1 Hirosawa, Wako, Saitama 351-0198, Japan*

A large variety of nanometre-scale devices have been investigated in recent years[1–7] that could overcome the physical and economic limitations of current semiconductor devices[8]. To be of technological interest, the energy consumption and fabrication cost of these 'nanodevices' need to be low. Here we report a new type of nanodevice, a quantized conductance atomic switch (QCAS), which satisfies these requirements. The QCAS works by controlling the formation and annihilation of an atomic bridge at the crossing point between two electrodes. The wires are spaced approximately 1 nm apart, and one of the two is a solid electrolyte

© 2005 Nature Publishing Group

wire from which the atomic bridges are formed. We demonstrate that such a QCAS can switch between 'on' and 'off' states at room temperature and in air at a frequency of 1 MHz and at a small operating voltage (600 mV). Basic logic circuits are also easily fabricated by crossing solid electrolyte wires with metal electrodes.

Mechanical relay switches were the main devices at the dawn of the computer age[9]. However, owing to limitations on their downsizing and operating speed, other devices have replaced them—first vacuum tubes, and then semiconductor devices. We have recently overcome the problems of mechanical switches by using atomic mechanics, which enables us to reduce the size of the device to the nanoscale while keeping the switching speed as fast as present-day electronic devices. Very small energy consumption is also promised, because the device works with a very small bias voltage (for example, 10 mV).

We found that a silver nano-protrusion can be formed at the surface of a silver sulphide (Ag_2S) crystal, which is a mixed ionic and electronic conductor[10], by a solid electrochemical reaction due to a tunnelling current[11,12]. Growth and shrinkage of the silver protrusion can be controlled by changing the polarity of the bias voltage applied to the material. The QCAS consists of a fixed Ag_2S electrode and a Pt electrode, with a spacing of about 1 nm. A grown silver protrusion forms an atomic bridge between the two electrodes when a positive bias is applied to the Ag_2S electrode. The conductance between the two electrodes then becomes very high, which means the device is switched on. By applying a negative bias to the Ag_2S electrode, the silver protrusion shrinks, thus breaking the atomic bridge, which switches the device off. At the early stage of this study, a scanning tunnelling microscope (STM) was used to make the 1-nm gap between the two electrodes[13]. However, use of a mechanical positioning system (for example, an STM) makes it difficult to use the QCAS as a component of actual devices.

Recently, we found that a QCAS can be formed at each crossing point when a Ag_2S-coated Ag wire is crossed by a Pt wire (Fig. 1a). The 'crossbar' structure is convenient for integrating switches to be used in actual devices[14], and we report here basic circuits using this structure. It would also produce a storage capacity of 2.5 Gbit cm^{-2} using the atomic switch even at the present level of miniaturization of the semiconductor industry. Since the atomic switch itself is much smaller than this level of miniaturization, much higher density could be made available by improving the miniaturization technology. The crossbar structure has been fabricated with a conventional nanofabricating method, which uses electron-beam lithography and related techniques such as metal deposition and lift-off. That is, Ag_2S-coated Ag wires are formed first by sulphurizing Ag wires. The sulphurization was done at 80 °C for 5 min in an ultrahigh vacuum by introducing sulphur vapour using a sulphur valved cracker cell. Then, Pt wires are formed across the Ag_2S-coated Ag wires.

The 1-nm gap, which is the key structure of the atomic switch, is made as follows. A 1-nm-thick Ag layer is deposited on the Ag_2S-coated Ag wires at the places where these wires are to be crossed by the Pt wires—this 1-nm-thick Ag layer is deposited before the formation of the Pt wires. Therefore, the switch is formed in the on state (Fig. 1b). Then, the switch is turned off by applying a certain positive bias voltage to the Pt electrode. Because of the larger amount of Ag atoms to be ionized for incorporating into the Ag_2S crystal in this first turning-off process, the switching time of this process is quite long (a few seconds). However, it becomes shorter after this initial operation.

The QCAS works stably at room temperature in a vacuum and even in air. No difference has been observed in the switching properties between operation in a vacuum and in air. We confirmed that it worked more than 10^5 times, and still continued to work showing constant switching properties—for example, threshold bias voltages and resistances both of the on and off states. We also confirmed that it can be formed by using other solid electrolytes such as Cu_2S, although we will only show here the results for the Ag_2S QCAS. The QCAS can be operated as fast as electronic devices. For instance, switching at 1 MHz by the atomic switch of the crossbar structure is shown in Fig. 2a. At present, switching times less than 1 μs cannot be measured, owing to the capacitance of the thick wires forming the QCAS, but we believe that it could work at 1 GHz, on the basis of the following experimental results on switching time.

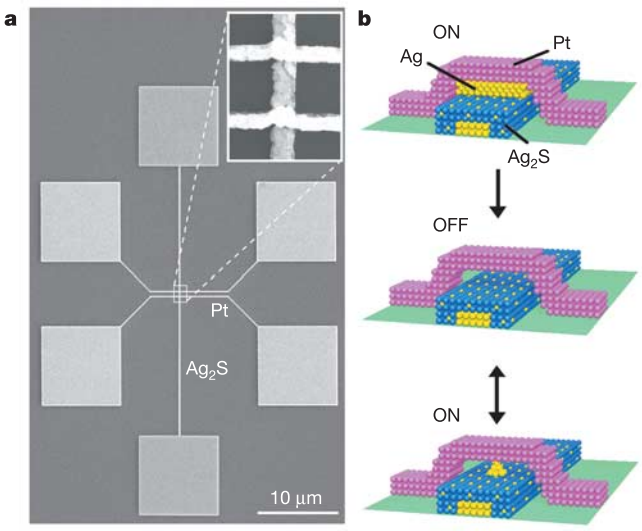

Figure 1 Basics of the QCAS. **a**, SEM image of the QCAS. A QCAS is formed at each crossing point of the 150-nm-wide Ag_2S wire and the two Pt wires of 100 nm width. **b**, Schematic diagrams of the QCAS. As-formed switched-on state (top), switched-off state (middle) and switched-on state after the initial switching-off process (bottom).

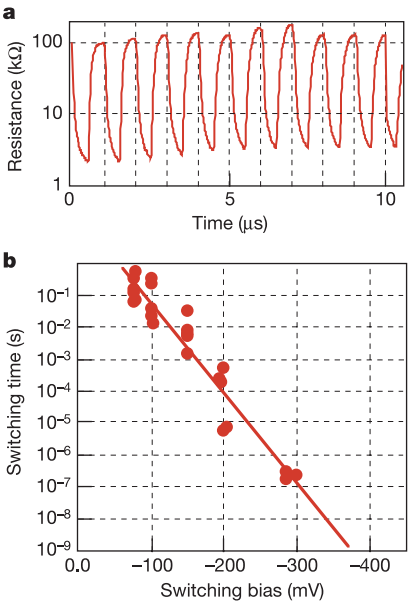

Figure 2 Switching results of the QCAS. **a**, Experimental result of switching at 1 MHz. Alternating switching bias voltages of ±600 mV were used. **b**, Time taken for the resistance of the QCAS to change from an 'off' resistance (100 kΩ) to an 'on' resistance (12.9 kΩ, which corresponds to $N = 1$ ($\times 2e^2/h$) of the quantized conductance) was measured with respect to the switching bias.

© 2005 Nature Publishing Group

Figure 2b shows the time it takes to switch on the device from the off state with a resistance of 100 kΩ. The result indicates that the switching time decreases exponentially with increasing switching bias voltage in the measured region. This exponential relation suggests that the solid electrochemical reaction, which has some activation energy[12], determines the switching speed. This result suggests that much faster switching could be achieved by using thin wires, which would enable us to apply a bias voltage of higher frequency to the switch. Since silver ions in the Ag_2S crystal are known[15] to be able to hop among the sites when responding to much higher frequencies than those we used, we believe that switching at 1 GHz, for instance, could be achieved with a bias voltage of 0.4 V. Operation as fast as conventional electronic devices could thus be possible, because only a small number of silver atoms have to be moved 1 nm at most for the switching to occur. In other words, downsizing the device to the atomic scale enables its fast operation.

Basic circuits, such as logic gates, have been made using the QCAS. For instance, an AND gate was made using two QCASs and a resistor (Fig. 3a). In the experiment, the crossbar structure having two QCASs (Fig. 1a) was connected to a macro resistor and a measuring system. Two input signals, V_1 and V_2, are applied to the Pt wires, and the output signal V_{out} was measured at one of the ends of the Ag_2S wire. According to the change in the two input signals, formation and annihilation of atomic bridges were controlled at both QCASs; the changes in the resistances of the two QCASs are shown in Fig. 3a. The operating result is also shown in Fig. 3a, where the output level becomes high only when both inputs are at the high level. By using the resistor, bias voltages effectively applied to the QCASs come into equilibrium soon after switching. In other words, the electrochemical reaction stops soon after each operation. Therefore, too many Ag atoms are not precipitated in each operation, which promises fast operation. The OR gate (Fig. 3b) and NOT gate (Fig. 3c) can be also configured. That all basic logic gates—that is, AND, OR and NOT—are configurable with QCASs means that any kind of logic circuit can be configured with QCASs.

In the operation of the logic gates, the QCAS is used as an on/off bistable switch. The quantized conductance that the QCAS shows can be also used to make circuits. This conductance is quantized with a unit of $2e^2/h$ (where e is the charge of the electron and h is Plank's constant), as observed in experiments using metal nanowires[16–24], as the width of the atomic bridge is comparable to the Fermi length of silver (0.52 nm). By controlling the tip position precisely, switching between quantized conductances has also been demonstrated[25]. However, the mechanical positioning systems (for example, an STM) employed in these studies make it difficult to use the quantized conductance property of nanowires in actual devices. Recently, a non-mechanical method for forming a nanowire using a liquid electrochemical reaction was proposed[26,27], which suggests the possibility of using a nanowire showing quantized conductance in conventional microelectronics.

Switching between quantized conductances of the QCAS is achieved by applying a pulsed bias voltage, which is larger than the threshold bias voltage of the electrochemical reaction[11,12]. A bias smaller than the threshold bias voltage is used to measure the conductance. Because of the clearness of conductance quantization in a nanowire with a small and completely fixed gap[28], the quantized conductance in the QCAS is much more controllable than that in other nanowires[16–24]. The conductances of multiple QCASs formed in an array are independently controllable. For instance, we controlled the conductances of a 1 × 2 array of QCASs, as shown in Fig. 4. In the experiment, we changed the conductances at each channel independently from $N = 0$ to 3 by using pulsed bias voltages (here N is the conductance in unit of $2e^2/h$). The total conductance, as calculated from the total current measured at the end of the silver wire, corresponds to the sum of the two conductances, which suggests that the system works as an adder circuit. It also works as a multi-state memory, as it memorizes 16 states simply by using two switches.

Though we have succeeded in demonstrating control of the quantized conductances, further work is needed before these quantized conductances can be used in actual devices. For instance, at this stage, higher numbers of quantized conductances are not as controllable as lower numbers. There is also a problem

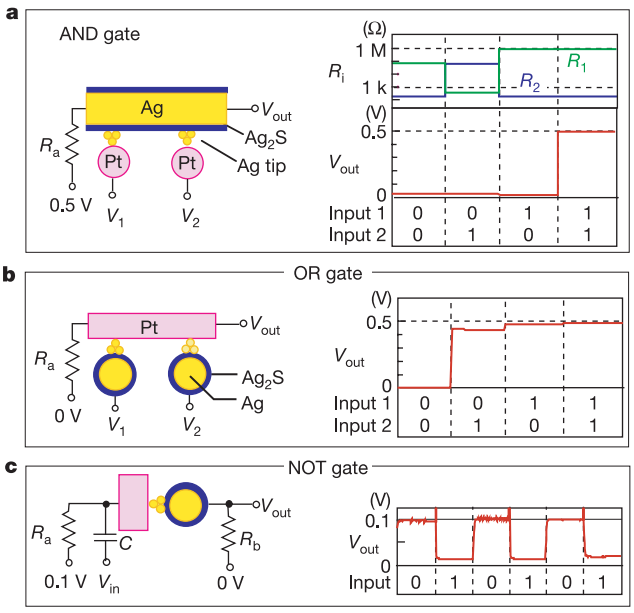

Figure 3 Logic gates configured with QCASs. **a**, Schematic diagram of an AND gate using QCASs (left) and its operating result (right). **b**, Schematic diagram of the OR gate (left) and its operating result (right). **c**, Schematic diagram of the NOT gate (left) and its operating result (right). Resistors R_a (10 kΩ) and R_b (1 kΩ), and a capacitor C (100 pF), are used. V_1 and V_2 are applied as input bias voltages. Input level 1 is 0.5 V for the AND and OR gates, and 1.5 V for the NOT gate. Input level 0 is 0 V for all gates. Input levels were changed every second.

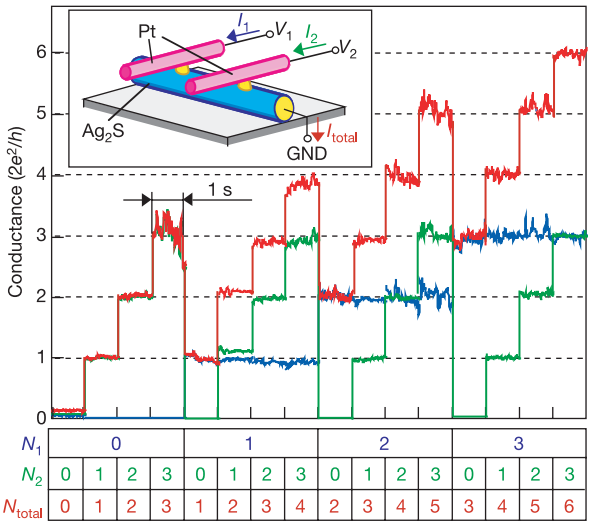

Figure 4 1 × 2 array of QCASs. The conductances of each channel were changed independently from $N = 0$ ($\times 2e^2/h$) to 3 ($\times 2e^2/h$). 50-ms-long pulsed bias voltages of 200 mV (from 0 to 1), 100 mV (from 1 to 2), 80 mV (from 2 to 3) and −260 mV (from 3 to 0) were used.

© 2005 Nature Publishing Group

with reproducibility even for smaller numbers of quantized conductances, because some switches are found to show less controllability—such as showing a non-integral N of 1.5. This is because the quantized conductance is strongly related to the atomic arrangement of the atomic bridge, which is difficult to control. Therefore, we think that the device structure needs to be improved before practical use of the quantized conductances can be made.

We believe that the simple structure, ease of operation, and the stability and reliability of the QCAS will enable us to use it as an element of future nanodevices, and to make conceptually new electronics that will be part of a new type of computer architecture[29]. In addition, the QCAS can be used as an element of present-day electronic devices, as the size of the switch itself is already at the atomic scale and it works efficiently at room temperature and in air. □

Received 1 September; accepted 18 November 2004; doi:10.1038/nature03190.

1. Tans, S. J., Verschueren, A. R. M. & Dekker, C. Room-temperature transistor based on a single carbon nanotube. *Nature* **393,** 49–52 (1998).
2. Martel, R., Schmidt, T., Shea, H. R., Hertel, T. & Avouris, Ph. Single- and multi-wall carbon nanotube field-effect transistors. *Appl. Phys. Lett.* **73,** 2447–2449 (1998).
3. Collier, C. P. *et al.* Electronically configurable molecular-based logic gates. *Science* **285,** 391–394 (1999).
4. Joachim, C., Gimzewski, J. K. & Aviram, A. Electronics using hybrid-molecular and mono-molecular devices. *Nature* **408,** 541–548 (2000).
5. Cui, Y. & Lieber, C. M. Functional nanoscale electronic devices assembled using silicon nanowire building blocks. *Science* **291,** 851–853 (2001).
6. Mathur, N. Beyond the silicon roadmap. *Nature* **419,** 573–575 (2002).
7. Duan, X. *et al.* High-performance thin-film transistors using semiconductor nanowires and nanoribbons. *Nature* **425,** 274–278 (2003).
8. Peercy, P. S. The drive to miniaturization. *Nature* **406,** 1023–1026 (2000).
9. Slater, R. *Portraits in Silicon* Ch. 3 & 13 (MIT Press, Cambridge, Massachusetts, 1989).
10. Kudo, T. & Fueki, K. *Solid State Ionics* 137–140 (Kodansha/VCH, Tokyo, 1990).
11. Terabe, K., Nakayama, T., Iyi, N. & Aono, M. in *Proc. 9th Int. Conf. on Production Engineering* (eds Furukawa, Y., Mori, Y. & Kataoka, T.) 711–716 (The Japan Society for Precision Engineering, Osaka, 1999).
12. Terabe, K., Nakayama, T., Hasegawa, T. & Aono, M. Formation and disappearance of a nanoscale silver cluster realized by solid electrochemical reaction. *J. Appl. Phys.* **91,** 10110–10114 (2002).
13. Terabe, K., Hasegawa, T., Nakayama, T. & Aono, M. Quantum point contact switch realized by solid electrochemical reaction. *Riken Rev.* **37,** 7–8 (2001).
14. Chen, Y. *et al.* Nanoscale molecular-switch devices fabricated by imprint lithography. *Appl. Phys. Lett.* **82,** 1610–1612 (2003).
15. Ohashi, K. & Ohashi, Y. H. Non-linear electrical transport in silver sulfide. *Solid State Ionics* **3/4,** 127–130 (1981).
16. Pascual, J. I. *et al.* Quantum contact in gold nanostructures by scanning tunneling microscopy. *Phys. Rev. Lett.* **71,** 1852–1855 (1993).
17. Olesen, L. *et al.* Quantized conductance in an atom-sized point contact. *Phys. Rev. Lett.* **72,** 2251–2254 (1994).
18. Costa-Kramer, J. L. *et al.* Conductance quantization in nanowires formed between micro- and macroscopic metallic electrodes. *Phys. Rev. B* **55,** 5416–5424 (1997).
19. Ohnishi, H., Kondo, Y. & Takayanagi, K. Quantized conductance through individual rows of suspended gold atoms. *Nature* **395,** 780–785 (1998).
20. Krans, J. M., Van Ruitenbeek, J. M., Fisun, V. V., Yansen, I. K. & de Jongh, L. J. The signature of conductance quantization in metallic point contacts. *Nature* **375,** 767–769 (1995).
21. Hansen, K., Læsgaard, E., Stensgaard, I. & Besenbacher, F. Quantized conductance in relays. *Phys. Rev. B* **56,** 2208–2220 (1997).
22. Agrait, N., Yeyati, A. L. & Ruitenbeek, J. M. Quantum properties of atomic-sized conductors. *Phys. Rep.* **377** (2–3), 81–279 (2003).
23. Enomoto, A., Kurokawa, S. & Sakai, A. Quantized conductance in Au-Pd and Au-Ag alloy nanocontacts. *Phys. Rev. B* **65,** 125410 (2002).
24. Rodrigues, V., Bettini, J., Rocha, A. R., Rego, L. G. C. & Ugarte, D. Quantum conductance in silver nanowires: correlation between atomic structure and transport properties. *Phys. Rev. B* **65,** 153402 (2002).
25. Smith, D. P. E. Quantum point contact switches. *Science* **269,** 371–373 (1995).
26. Li, C. Z. & Tao, N. J. Quantum transport in metallic nanowires fabricated by electrochemical deposition/dissolution. *Appl. Phys. Lett.* **72,** 894–896 (1998).
27. Xu, B., He, H. & Tao, N. J. Controlling the conductance of atomically thin metal wires with electrochemical potential. *J. Am. Chem. Soc.* **124,** 13568–13575 (2002).
28. Oshima, Y., Mouri, K., Hirayama, H. & Takayanagi, K. Development of a miniature STM holder for study of electronic conductance of metal nanowires in UHV-TEM. *Surf. Sci.* **531,** 209–216 (2003).
29. Heath, J. R., Kuekes, P. J., Snider, G. S. & Williams, R. S. A defect-tolerant computer architecture: opportunities for nanotechnology. *Science* **280,** 1716–1721 (1998).

Acknowledgements We thank M. Kundu and R. Negishi for fabrication of the crossbar-type switches, and T. Tamura for help with measurement of the switching time.

Competing interests statement The authors declare that they have no competing financial interests.

Correspondence and requests for materials should be addressed to T.H. (HASEGAWA.Tsuyoshi@nims.go.jp).

Increasing the conductivity of crystalline polymer electrolytes

Alasdair M. Christie, Scott J. Lilley, Edward Staunton, Yuri G. Andreev & Peter G. Bruce

School of Chemistry, University of St Andrews, St Andrews KY16 9ST, UK

Polymer electrolytes consist of salts dissolved in polymers (for example, polyethylene oxide, PEO), and represent a unique class of solid coordination compounds. They have potential applications in a diverse range of all-solid-state devices, such as rechargeable lithium batteries, flexible electrochromic displays and smart windows[1–5]. For 30 years, attention was focused on amorphous polymer electrolytes in the belief that crystalline polymer:salt complexes were insulators. This view has been overturned recently by demonstrating ionic conductivity in the crystalline complexes PEO_6:$LiXF_6$ (X = P, As, Sb); however, the conductivities were relatively low[6,7]. Here we demonstrate an increase of 1.5 orders of magnitude in the conductivity of these materials by replacing a small proportion of the XF_6^- anions in the crystal structure with isovalent $N(SO_2CF_3)_2^-$ ions. We suggest that the larger and more irregularly shaped anions disrupt the potential around the Li^+ ions, thus enhancing the ionic conductivity in a manner somewhat analogous to the $AgBr_{1-x}I_x$ ionic conductors[8]. The demonstration that doping strategies can enhance the conductivity of crystalline polymer electrolytes represents a significant advance towards the technological exploitation of such materials.

Ionic conductivity in polymer electrolytes was believed to occur in a manner somewhat analogous to gas diffusion through polymer membranes. Segmental motion of the polymer chains continuously creates free volume into which the ions migrate, and this process allows them to progress across the electrolyte[1–3,9]. Such a view was established by a number of experiments, and denied the possibility of ionic conductivity in crystalline polymers[10,11]. As a result, attention for the past 30 years has concentrated on amorphous polymer electrolytes, and in particular on the synthesis of new materials with low T_g (glass transition temperature) and hence high levels of segmental motion in order to increase the conductivity[12].

Polymer electrolytes may be prepared as either amorphous or crystalline materials, the latter at certain discrete compositions (ether oxygen to salt ratios). As part of a programme devoted to investigating the structures of the crystalline polymer electrolyte complexes, we solved the crystal structures of the 6:1 complexes PEO_6:$LiXF_6$ (X = P, As, Sb), and recognized that they had the features necessary to support ionic conductivity in the crystalline state. The structures of the three 6:1 complexes are broadly similar, and are composed of pairs of PEO chains that fold together to form tunnels within which the Li^+ ions reside: the anions are located outside the tunnels[13]. Subsequently, we demonstrated that these were ionically conducting crystalline polymer electrolytes[6,7]. Although this was an important development, the conductivities of these materials were low at room temperature (typically $10^{-7}\,S\,cm^{-1}$). For applications, it is essential to find ways of raising the conductivity. Smart windows and electrochromic displays do not require conductivities as high as those needed for lithium batteries, but values in excess of $10^{-7}\,S\,cm^{-1}$ are essential. We have discovered that it is possible to replace up to 5 mol% of the AsF_6^- ions in the PEO_6:$LiAsF_6$ crystal structure by the isovalent $N(SO_2CF_3)_2^-$ (bis(trifluoromethanesulphonyl)imide or TFSI) ions, resulting in an enhancement in conductivity of 1.5 orders of magnitude. Attempts to replace more AsF_6^- ions resulted in a

© 2005 Nature Publishing Group